LINEAR MODEL FOR CANAL POOLS

João Miguel Lemos Chasqueira Nabais
Department of Systems and Informatics, Escola Superior de Tecnologia de Setúbal
Campus do IPS, Estefanilha 2910-761 Setúbal, Portugal

Miguel Ayala Botto
Department of Mechanical Engineering, IDMEC, Instituto Superior Técnico
Av. Rovisco Pais, 1049-001 Lisboa, Portugal

Keywords: Modeling, Partial differential equations, Saint-Venant equations, Open-channels, Water conveyance systems, Time delay system, Fault tolerant control.

Abstract: Water is vital for human life.Water is used widespread from agricultural to industrial as well as simple domestic activities. Mostly due to the increase on world population, water is becoming a sparse and valuable resource, pushing a high demand on the design of efficient engineering water distribution control systems. This paper presents a simple yet sufficiently rich and flexible solution to model open-channels. The hydraulic model is based on the Saint-Venant equations which are then linearized and transformed into a state space dynamic model. The resulting model is shown to be able to incorporate different boundary conditions like discharge, water depth or hydraulic structure dynamics, features that are commonly present on any water distribution system. Besides, due its computational simplicity and efficient monitoring capacity, the resulting hydraulic model is easily integrated into safety and fault tolerant control strategies. In this paper the hydraulic model is successfully validated using experimental data from a water canal setup.

1 INTRODUCTION

Water is an essential resource for all life species, in particular human life. From agricultural to industrial applications or simple domestic activities, an efficient water conveyance network is a key factor for a sustainable development, social stability and welfare. Water can be distributed through natural irrigation canals provided by nature itself, like rivers, or be either transported by means of artificial irrigation canals generally known as water conveyance systems. These systems have usually great complexity from an automatic control point of view, since they are generally large spatially distributed systems with strong nonlinearities and physical constraints, time delays, while their operation typically requires the compatibility of multiple competing objectives. Therefore the need for an accurate dynamic hydraulic model that is sufficiently rich to incorporate the most relevant physical dynamics, while being flexible enough to be adapted to different operational setups.

For model base canal controller design is necessary to have a good model able to capture the main system dynamics. A simple analytical model was proposed by (Schuurmans et al., 1995) the so-called integrator delay whose simplicity made it popular for canal modeling (Schuurmans et al., 1999b) (Schuurmans et al., 1999a). Although being a simple model, controller design using this type of model is still a current research topic (van Overloop, 2006; Negenborn et al., 2009). If more accuracy is needed then Saint Venant equations (Akan, 2006) are commonly used to model the dynamic behavior of the water flow in open water canals. The Saint-Venant equations consist of a pair of nonlinear hyperbolic partial differential equations. These equations are hard to be handled and so typically a linearized version around an equilibrium point is used for simulation and control purposes (Litrico and Fromion, 2002). In (Litrico and Fromion, 2009) it is shown how a continuous multivariable dynamic model relating inflows to water depths for an open water pool is obtained. This model is specially suitable for H_∞ frequency analysis. Based on this structure, a simplified single-input single-output Integral Delay Zero (IDZ) model was shown to capture the main hydraulic dynam-

Miguel Lemos Chasqueira Nabais J. and Ayala Botto M..
LINEAR MODEL FOR CANAL POOLS.
DOI: 10.5220/0003536103060313
In *Proceedings of the 8th International Conference on Informatics in Control, Automation and Robotics* (ICINCO-2011), pages 306-313
ISBN: 978-989-8425-74-4

ics (Litrico and Fromion, 2004). However, although simple, the IDZ model lacks some accuracy (Nabais and Botto, 2010). A more flexible model framework that is computationally simple with efficient monitoring capacity of the canal water depths is then required.

This paper presents a discrete-time linear state space model for canal pools. The model is obtained through the discretization of the linearized Saint-Venant equations around a stationary point. The following interesting features can be found:

- a minimum computational effort is required for simulation purposes making it easily extendable to high dimensional open water networks;
- monitoring water depths and discharges along the canal can be easily made through an appropriate choice of the output equation;
- boundary conditions are easily integrated as discharges or water depths, allowing for modular interconnection of different elements on a given open water canal;
- it enables the accommodation of hydraulic structure dynamics to which the pool is linked to;
- it can be easily integrated into model based control strategies (Martinez, 2007) (Silva et al., 2007) opening the gate to its inclusion in fault tolerant control applications (Blanke et al., 2006) (Isermann, 2006) (Bedjaoui et al., 2009).

Besides, the proposed hydraulic model is further validated against real data retrieved from an experimental water delivery canal hold by the NuHCC – Hydraulics and Canal Control Center from the Évora University in Portugal.

The paper has the following structure. Section 2 presents the experimental canal. The canal model problem formulation is then presented in section 3 where the partial differential dynamic equations describing the transport phenomenon are first linearized and then discretized leading to a finite linear pool model. In section 4 a brief model numerical parameter analysis is presented. In section 5 the hydraulic model is validated with data retrieved from the experimental canal. Here it is shown the reliability and accuracy of the proposed hydraulic model. Finally, in section 6 some conclusions are drawn.

2 EXPERIMENTAL CANAL

The experimental automatic canal is located in Mitra near Évora, Portugal (Figure 1). The canal has 4 pools with a trapezoidal cross section of 0.900m height, 0.150m bottom width b and a side slope of

Figure 1: Experimental canal global view.

Table 1: Experimental canal uniform parameters.

Parameter	Pool 1	Pool 2	Pool 3	Pool 4
L [m]	40.7	35	35	35.2
S_0	0.0016	0.0014	0.0019	0.0004
n [$m^{-1/3}s$]	0.015	0.015	0.015	0.015
b [m]	0.15	0.15	0.15	0.15
m [m]	1:0.15	1:0.15	1:0.15	1:0.15

$m = 1 : 0.15$. The geometric characteristics for each pool are shown in Table 1 where L means pool length, S_0 the bed slope and n the Manning friction coefficient.

The 4 pools are divided by three sluice gates as shown in Figure 2. All theses sluice gates are electro-actuated and instrumented with position sensors. A rectangular overshot gate is located at the end of the canal with 0.38m width. The off-take valves, equipped with an electromagnetic flowmeter and motorized butterfly valve for flow control, are immediately located upstream of each sluice gate. Counterweight-float level sensors are distributed along the canal.

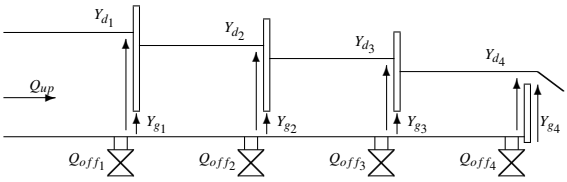

Figure 2: Schematics of the complete facility.

At the head of the canal an electro-valve controls the canal inflow. This flow is extracted from a reservoir. The maximum flow capacity is 0.090 m^3/s. The flow within the automatic canal is regulated by another electro-valve located at the exit of a high reservoir (head of the automatic canal), simulating a real load situation. This high reservoir is filled with the recovered water pumped from a low one, which collects the flow from a traditional canal

allowing a closed circuit. All electro-actuators and sensors in the canal are connected to local PLCs (Programmable Logic Controllers) responsible for the sensor data acquisition and for the control actions sent to the actuators (Almeida et al., 2002). All local PLCs are connected through a MODBUS network (RS 485). The interaction with the Évora canal is done through 5 inputs (canal intake Q_{up} and 4 gate positions Y_{g_i}), 4 outputs (downstream water level at each pool Y_{L_i}) and 4 considered disturbances Q_{off_i}(offtakes at each pool end) using a multi-platform controller interface (Duarte et al., 2011).

3 CANAL POOL MODEL

3.1 First Principles

The flow in open-channels is well described by the Saint-Venant equations,

$$\frac{\partial Q(x,t)}{\partial x} + B(x,t)\frac{\partial Y(x,t)}{\partial t} = 0 \quad (1)$$

$$\frac{\partial Q(x,t)}{\partial t} + \frac{\partial}{\partial x}\left(\frac{Q^2(x,t)}{A(x,t)}\right) + \ldots$$
$$\ldots + g \cdot A(x,t) \cdot (S_f(x,t) - S_0(x)) = 0 \quad (2)$$

where, $A(x,t)$ is the wetted cross section, $Q(x,t)$ is the water discharge, $Y(x,t)$ is the water depth, $B(x,t)$ is the wetted cross section top width, $S_f(x,t)$ is the friction slope, $S_0(x)$ is the bed slope, x and t are the independent variables. These equations are partial differential equations of hyperbolic type capable of describing the transport phenomenon. The mathematical dynamical model used is known for being able to capture the process physics namely: backwater, wave translation, wave attenuation and flow acceleration.

To solve partial differential equations it is necessary to know the initial condition along the canal axis and also two boundary conditions in time.

3.1.1 Initial Conditions

The flow can be classified according to the independent variables variations in time and space:

- uniform flow, when parameters do not vary along canal axis, nonuniform when parameters vary in space,
- steady flow, when parameters do not vary in time, and unsteady when parameters vary in time.

In this paper the *Nonuniform Unsteady Flow* is assumed. One interesting situation is to consider gradually varied flow. This is characterized for steady conditions, which means $\frac{\partial}{\partial t} = 0$. In this case the Saint-Venant equations are reduced to Ordinary Differential Equation. If also uniform flow is to be imposed, no variations along canal axis, it is only necessary to solve $S_f(x,t) = S_0(x)$. The water depth found is also known as the normal depth Y_N. If a downstream water condition different from the normal depth is given then the water profiles presented in Figure 3 result.

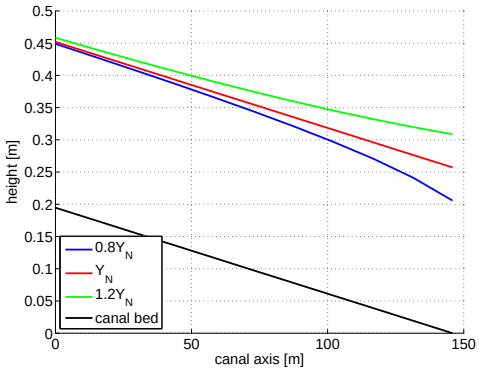

Figure 3: Backwater for some downstream water depths with a nominal discharge of $Q_0 = 0.020\text{m}^3/\text{s}$.

3.1.2 Boundary Conditions

Partial differential equations of hyperbolic type are capable of describing the transport phenomenon. There are two waves presented in the pool dynamics whose velocity are $V + C$ and $V - C$, where V is average velocity across section and C is the wave celerity. Depending on the relation between the dynamical and inertial velocity captured by the Froude number, $F_r = \frac{V}{C}$ the flow can be characterized into the following three types:

- subcritical: for $F_r < 1$ designated as fluvial and is typical of large water depths and small discharge and can be found at the river downstream,
- critical: for $F_r = 1$,
- supercritical: for $F_r > 1$ designated as torrential and is typical for small depth and large discharge and can be found at the river upstream.

In the subcritical case two waves traveling in opposite direction along the canal axis may occur. Because of this phenomenon, one boundary condition at each pool end is needed. In this paper only subcritical flow is considered.

3.2 PDE Resolution

For solving numerically the partial differential equation it is required to proceed with time and space dis-

cretization. Here two approaches are valid (Litrico and Fromion, 2009):

- Hydraulic approach: in this classical approach the equations are first discretized and then the non-linear terms are approximated. This leads to time variant systems and requires the resolution of a set of algebraic equations, for instance through the generalized Newton method,
- Control approach: in this approach the equations are first linearized around a stationary configuration $(Q_0, Y_0(x))$. After this step the equations are discretized which allows for a time invariant state space representation.

Consider a steady state defined as $(Q_0, Y_0(x))$ where index 0 stands for steady flow configuration. The deviation variables are defined as,

$$\begin{aligned} q(x,t) &= Q(x,t) - Q_0 \\ y(x,t) &= Y(x,t) - Y_0(x) \end{aligned}$$

Assuming $A(x,t) = B_0(x)Y(x,t)$, after linearization equations (1) (2) become,

$$B_0(x)\frac{\partial y(x,t)}{\partial t} + \frac{\partial q(x,t)}{\partial x} = 0 \quad (3)$$

$$\frac{\partial q(x,t)}{\partial t} + 2V_0(x)\frac{\partial q(x,t)}{\partial x} + \delta(x)q(x,t) + \ldots$$
$$+ \left[C_0^2(x) - V_0^2(x)\right] B_0(x)\frac{\partial y(x,t)}{\partial x} - \tilde{\gamma}(x)y(x,t) = 0 \quad (4)$$

where,

$$\begin{aligned} C_0(x) &= \sqrt{g\frac{A_0(x)}{B_0(x)}} \\ \alpha(x) &= C_0(x) + V_0(x) \\ \beta(x) &= C_0(x) - V_0(x) \\ \delta(x) &= \frac{2\cdot g}{V_0(x)}\left(J_0(x) - Fr_0^2(x)\frac{dY_0(x)}{dx}\right) \\ Fr_0^2(x) &= \frac{V_0^2(x)B_0(x)}{g\cdot A_0(x)} \\ \tilde{\gamma}(x) &= V_0^2(x)\frac{dB_0(x)}{dx} + g\cdot B_0(x)\left[D(x)J_0(x) + \ldots\right. \\ &\quad \left. + I(x) - \left(1 + 2Fr_0^2(x)\right)\frac{dY_0(x)}{dx}\right] \\ D(x) &= \frac{7}{3} - \frac{4}{3}\frac{A_0(x)}{P_0(x)B_0(x)}\frac{\partial P_0(x)}{\partial y} \end{aligned} \quad (5)$$

To complete the linearized pool model it is necessary to consider an initial condition along the spatial coordinate,

$$q(x,0) = q_0(x) = q_0 \quad y(x,0) = y_0(x) \quad (6)$$

and two boundary conditions on each end along time,

$$q(0,t) = u_1(t) \quad q(L,t) = u_2(t) \quad (7)$$

To simplify future analysis the Saint-Venant equations can be re-written into a more convenient alternative form. For that consider the area deviation as $a(x,t) = B_0(x)y(x,t)$. The linearized equations (3) and (4) are now given by,

$$\frac{\partial a(x,t)}{\partial t} + \frac{\partial q(x,t)}{\partial x} = 0 \quad (8)$$

$$\frac{\partial q(x,t)}{\partial t} + \left[\alpha(x) - \beta(x)\right]\frac{\partial q(x,t)}{\partial x} + \ldots$$
$$+\alpha(x)\beta(x)\frac{\partial a(x,t)}{\partial x} + \delta(x)q(x,t) - \gamma(x)a(x,t) = 0 \quad (9)$$

where,

$$\gamma(x) = \frac{C_0^2(x)}{B_0(x)}\frac{dB_0(x)}{dx} + g\left[(1 + D(x))I(x) + \ldots\right.$$
$$\left. - \left(1 + D(x) - (D(x) - 2)Fr_0^2(x)\right)\frac{dY_0(x)}{dx}\right] \quad (10)$$

Considering the state vector $\chi(x,t) = \begin{bmatrix} q(x,t) & a(x,t) \end{bmatrix}^T$ equations (8) and (9) may be expressed in state space form as follows,

$$A\frac{\partial}{\partial t}\chi(x,t) + B(x)\frac{\partial}{\partial x}\chi(x,t) + C(x)\chi(x,t) = 0 \quad (11)$$

where,

$$\begin{aligned} A &= \begin{bmatrix} 0 & 1 \\ 1 & 0 \end{bmatrix} \\ B(x) &= \begin{bmatrix} 1 & 0 \\ \alpha(x) - \beta(x) & \alpha(x)\beta(x) \end{bmatrix} \\ C(x) &= \begin{bmatrix} 0 & 0 \\ \delta(x) & -\gamma(x) \end{bmatrix} \end{aligned} \quad (12)$$

3.3 Finite Dimension Model

The numerical method used to obtain a finite dimension model is the implicit method known as Preissmann Scheme. In this method Δx is the spatial mesh dimension, Δt is the time step, θ and ϕ weighting parameters ranging from 0 to 1. When using numerical methods it is important to be aware that they may introduce nonphysical behavior that is similar to the process physics and once introduced is not clear how to eliminate it (Szymkiewicz, 2010).

The state vector for two consecutive sections is fourth dimension with both upstream and downstream discharge and area deviation, $x(k) = \begin{bmatrix} q_i^k & a_i^k & q_{i+1}^k & a_{i+1}^k \end{bmatrix}^T$, where index k stands for time and index i stands for space. Applying the Preissmann scheme to equation (11) after some manipulations the following discrete state space representation is obtained,

$$\begin{bmatrix} a_{11} & a_{21} \\ a_{12} & a_{22} \\ a_{13} & a_{23} \\ a_{14} & a_{24} \end{bmatrix}^T \begin{bmatrix} q_i^{k+1} \\ a_i^{k+1} \\ q_{i+1}^{k+1} \\ a_{i+1}^{k+1} \end{bmatrix} + \ldots$$

$$\ldots + \begin{bmatrix} b_{11} & b_{21} \\ b_{12} & b_{22} \\ b_{13} & b_{23} \\ b_{14} & b_{24} \end{bmatrix}^T \begin{bmatrix} q_i^{k} \\ a_i^{k} \\ q_{i+1}^{k} \\ a_{i+1}^{k} \end{bmatrix} = 0 \quad (13)$$

The state space representation describes the pool dynamics between two adjacent sections. To obtain the model corresponding to a pool divided into N reaches it is necessary to use $N+1$ sections leading to $2(N+1)$ variables. Using model (13) is possible to obtain $2N$ equations. The last two equations are related to the upstream and downstream boundary conditions. The boundary conditions are imposed normally by the structure the pool is linked to. The boundary condition may be imposed in discharge, usually when connected to gates, or in water depth, when the pool is connected to large reservoirs. A slightly more complex approach is when some hydraulic structure dynamics are to be incorporated into the model. The hydraulic structure linearized equation is used as a boundary condition. In this case a local linear model is constructed describing the pool plus gate dynamics. With this approach the entire open water canal dynamics can be obtained by means of connection local model dynamics, also called linear agents. These linear agents may be used for local model base control strategies.

In this paper discharge boundary conditions are assumed for constructing an open water canal simulator with the objective of validating the Saint-Venant resolution method proposed.

The total pool state vector $\mathbf{X}(k)$ is defined as,

$$\mathbf{X}(k) = \begin{bmatrix} q_1(k) & a_1(k) & q_2(k) & a_2(k) & \ldots \\ \ldots & q_n(k) & a_n(k) & q_{n+1}(k) & a_{n+1}(k) \end{bmatrix} \quad (14)$$

Finally, the water pool linear model representation can be given as,

$$\begin{aligned} \mathbf{X}(k+1) &= A\mathbf{X}(k) + B\mathbf{U}(k) \\ \mathbf{Y}(k) &= C\mathbf{X}(k) \end{aligned} \quad (15)$$

where $\mathbf{U}(k)$ is the model input and $\mathbf{Y}(k)$ is the model output. It is important to emphasize some features of this model: i) the partial differential equations are solved only by matrices multiplications; ii) the number N of reaches inside a pool defines the number of sections $N+1$ and state space variables $2(N+1)$; and iii) all state space variables are accessible through matrix C in the output equation.

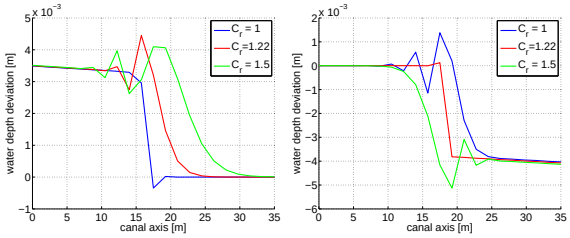

Figure 4: Wave propagation for different time step values.

4 PARAMETER ANALYSIS

The use of numerical methods for simulation may well introduce numerical oscillations and diffusion which, at the worst case, can lead to instability. Numerical methods are also known for introducing non physical dynamics which are similar to the process dynamics. After a finite dimension model is obtained, it is then crucial to proceed with parameters analysis. It is important to know how the nominal model performance is affected by the numerical parameters. This evaluation will be done for wave propagation along canal axis created by imposing a positive step input discharge at the boundary condition. The analysis is made for the second canal pool.

The nominal model was built with the following parameters: $L = 35\text{m}$ $N = 20$, $\Delta x = \frac{L}{N}$, $\Delta t \rightarrow C_r \approx 1$, $\phi = 0.5$ and $\theta = 0.5$, where C_r means the Courant number defined as,

$$C_r = \alpha \frac{\Delta t}{\Delta x} \quad (16)$$

which can be seen as the ratio between numerical velocity and kinematic velocity.

4.1 Sample Time

The sample time is one of the grid dimension parameters. Reducing it means that the numerical solution is calculated faster than the dynamical velocity. As a consequence the Courant number is reduced. Different Courant numbers tested are, $C_r = \begin{bmatrix} 1 & 1.22 & 1.5 \end{bmatrix}$ or in time step $\Delta t = \begin{bmatrix} 0.835 & 1.02 & 1.25 \end{bmatrix}$. In Figure 4 two waves travelling along canal axis for a given time instant are shown. It is clear that the system exhibits nonphysical oscillations that are not damped by the sample time.

Time step is not a tunable parameter. It must be chosen to keep the Courant number close to unity in order to have similar resolution in time and space. Contrary to what happens in continuous systems, reducing the time step does not improve the numerical solution.

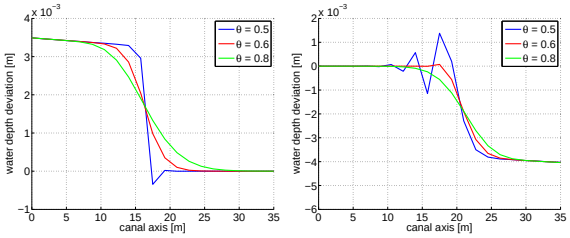

Figure 5: Wave propagation for different θ values.

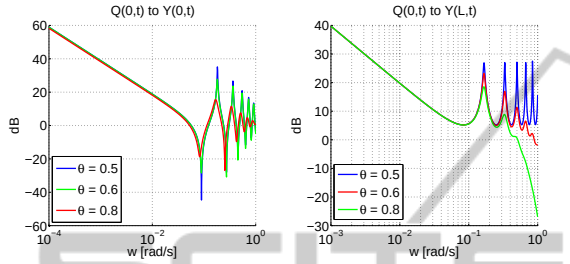

Figure 6: Frequency response for different θ values.

4.2 Preissmann Parameters

A centered approach in space is used, which means $\phi = 0.5$. Only the interpolation parameter in time θ is changed. The centered scheme is known to be unconditionally stable for $\theta \geq 0.5$. The following values were tested $\theta = \begin{bmatrix} 0.5 & 0.6 & 0.8 \end{bmatrix}$. In Figure 5 the downstream and upstream wave propagation when a positive discharge step is applied at the pool end is shown.

The effect of increasing the θ parameter is similar: numerical oscillations are eliminated at the cost of introducing numerical diffusion. This interpretation can be confirmed in the frequency response represented in Figure 6 for the upstream discharge input.

The first natural frequency is kept almost unchanged while the higher frequencies are damped. Although these parameters allow for numerical oscillations elimination it may introduce too much diffusion in the model.

4.3 Space Step

The space step is related to the number of reaches N considered in a pool. Assuming uniform space step parameter along canal axis it is practical to use $\Delta x = \frac{L}{N}$. If more resolution in the canal is desired this is the parameter to change, through the number of reaches. This is important as the space step is a constraint to the capacity of representing smaller waves as well as more abrupt changes in water profile. In Figure 7 the downstream and upstream wave propagation when a positive discharge step is applied at the pool end is shown. Establishing the N parameter is a tradeoff between accuracy and model complexity.

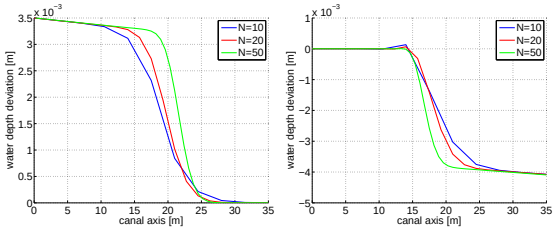

Figure 7: Wave propagation for different N values.

5 MODEL VALIDATION

The model validation is done using data collected from the experimental canal. To emphasize the canal monitoring ability the canal configuration with the intermediate gates opened is used. In this case the canal is a single pool of 145.9m length. The initial condition used was $Q_0 = 0.045\text{m}^3/\text{s}$ and $Y_0(L) = 0.595\text{m}$ with the associated gate opening $Y_g = 0.430\text{m}$. The linear pool model was constructed considering $N = 10$, $\theta = 0.6$ and a Courant number close to unity. In this configuration the Évora canal admits two inputs, a distant upstream discharge and a local gate opening.

Three different input scenarios were created for model validation, *test 1* – only upstream inflow, *test 2* – only local gate opening and *test 3* – with both inputs. The scenarios run over approximately 8000s which is equivalent to 2hours and 15minutes. The input sequence was designed accordingly to the Évora canal specifications. For the inflow the interval $[0.030; 0.045]\text{m}^3/\text{s}$ is tested, leading to a maximum deviation of 33% relative to Q_0. For the gate opening the interval $[0.330; 0.480]\text{m}$ is tested leading to a maximum deviation of 23% relative to $Y_0(L)$. The input sequence for test 3 is represented in Figure 8. In Figure 9 the canal backwater is drawn for the upper and lower hydraulic stationary configuration.

In Figure 10–12 the system output – the downstream water depth – and three more water depths along the canal axis are shown, which proves the model canal axis monitoring ability. One is considering $x = 1/4L$, $x = 1/2L$ and $x = 3/4L$.

In Table 2 the error criteria for downstream water depth as well for the intermediate points is presented. The error measurements used are the Variance Accounted For (VAF) and the Mean Absolute Error (MAE), the index refers to the test. The discharge input causes small variation in downstream water depth while the opening gate is more severe. The lowest fit occurs at the downstream end, which can be ex-

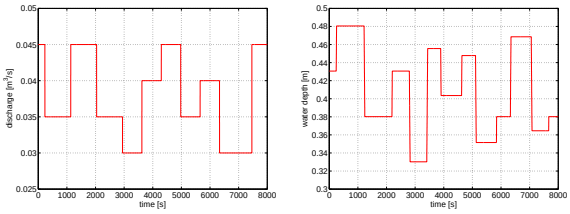

(a) Test 1 inflow. (b) Test 2 opening gate.

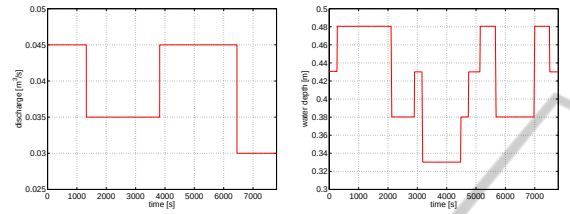

(c) Test 3 inflow. (d) Test 3 opening gate.

Figure 8: Tests input sequence.

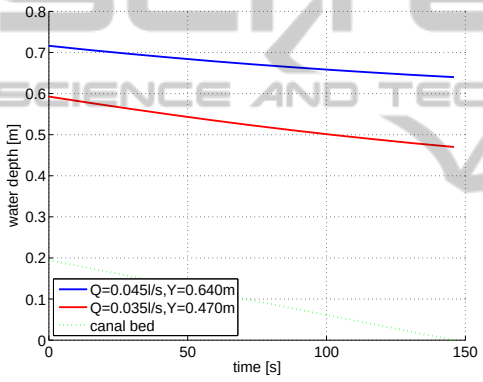

Figure 9: Backwater for upper and lower hydraulic steady flow configuration during the tests.

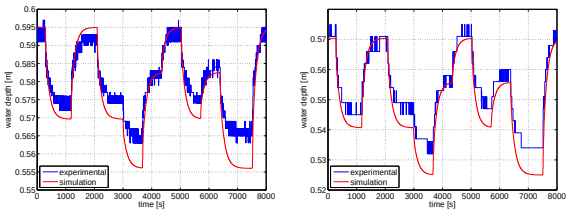

(a) $x = L$. (b) $x = 3/4L$.

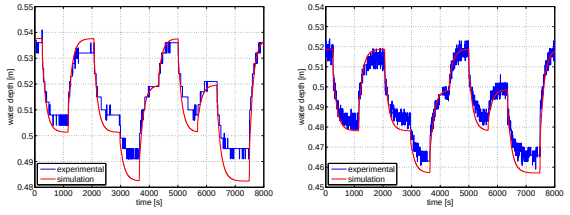

(c) $x = 1/2L$. (d) $x = 1/4L$.

Figure 10: Water depths for test 1.

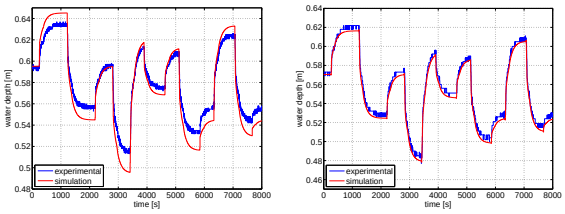

(a) $x = L$. (b) $x = 3/4L$.

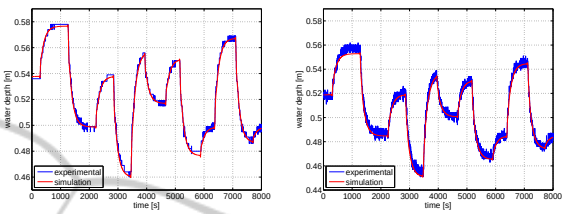

(c) $x = 1/2L$. (d) $x = 1/4L$.

Figure 11: Water depths for test 2.

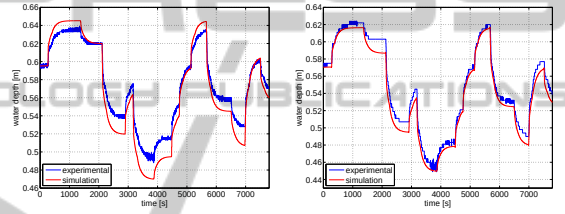

(a) $x = L$. (b) $x = 3/4L$.

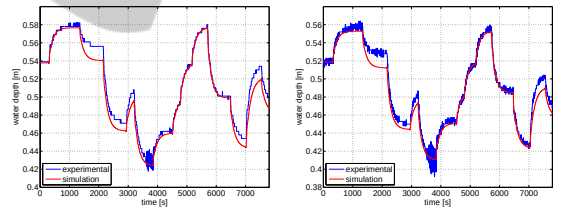

(c) $x = 1/2L$. (d) $x = 1/4L$.

Figure 12: Water depths for test 3.

plained by the experimental canal construction. The canal ends with a final reach of 7m length with rectangular section and 0.7m width. This is different from the nominal parameters considered and changes the downstream reservoir capacity.

It is important to note that while in test 1 the water depth amplitude varies 0.030 m in test 3 due to the gate movement, a water depth amplitude variation of 0.170 m is observed, which is quite large when compared with the nominal downstream water depth.

A similar model validation was done for a model with $N = 30$ which means a space step of 5m but no increase in performance was obtained. However the computationally cost was severely increased.

Table 2: Model criteria error for the different tests.

Canal axis	VAF_1	VAF_2	VAF_3
$x = L$	80.36	91.14	91.97
$x = 3/4L$	91.71	99.61	99.29
$x = 1/2L$	87.43	99.58	98.50
$x = 1/4L$	93.40	99.09	98.37
Canal axis	MAE_1	MAE_2	MAE_3
$x = L$	0.0041	0.0092	0.0121
$x = 3/4L$	0.0066	0.0061	0.0097
$x = 1/2L$	0.0049	0.0019	0.0064
$x = 1/4L$	0.0053	0.0040	0.0074

6 CONCLUSIONS

A finite dimension linear model for canal pools has been presented and validated with experimental data. The linearized partial differential equations describing the system are solved through matrices multiplications which requires low computational effort. This enables the model to be used for constructing open water network systems. The possibility to use the discharge, water depth or linearized hydraulic structures as boundary conditions, augments the model applicability.

The proposed model also allows for full canal monitoring. This is an important feature that opens the scope of application to fault detection, isolation, and fault tolerant control algorithms.

ACKNOWLEDGEMENTS

This work was co-sponsored by project AQUANET - Decentralized and Reconfigurable Control for Water delivery Multipurpose Canal Systems (PTDC/EEA-CRO/102102/2008), FCT, Portugal, through IDMEC by the Associated Laboratory in Energy, Transports, Aeronautics and Space.

REFERENCES

Akan, A. O. (2006). *Open Channel Hydraulics*. Elsevier.

Almeida, M., ao Figueiredo, J., and Rijo, M. (2002). Scada configuration and control modes implementation on an experimental water supply canal. In *10th Mediterranean Conference on Control Automation*, Lisbon, Portugal.

Bedjaoui, N., Weyer, E., and Bastin, G. (2009). Methods for the localization of a leak in open water channels. *Networks and Heterogeneous Media*, 4(2):180–210.

Blanke, M., Kinnaert, M., Lunze, J., and Staroswiecki, M. (2006). *Diagnosis and Fault-Tolerant Control*. Springer-Verlag.

Duarte, J., Rato, L., Shirley, P., and Rijo, M. (2011). Multiplatform controller interface for scada application. In *IFAC World Congress (Accepted in)*, Milan, Italy.

Isermann, R. (2006). *Fault-Diagnosis Systems*. Springer-Verlag.

Litrico, X. and Fromion, V. (2002). Infinite dimensional modelling of open-channel hydraulic systems for control purposes. In *41th IEEE Conference on Decision and Control*, pages 1681–1686, Las Vegas, Nevada.

Litrico, X. and Fromion, V. (2004). Simplified modeling of irrigation canals for controller design. *Journal of Irrigation and Drainage Engineering*, 130:373–383.

Litrico, X. and Fromion, V. (2009). *Modeling and Control of Hysrosystmes*. Springer-Verlag.

Martinez, C. A. O. (2007). *Model Predictive Control of Complex Systems including Fault Toelrance Capabilities: Application to Sewer Networks*. PhD thesis, Technical University of Catalonia.

Nabais, J. and Botto, M. A. (2010). Qualitative comparison between two open water canal models. In *9th Portuguese Conference on Automatic Control*, pages 501–506, Coimbra, Portugal.

Negenborn, R., van Overloop, P.-J., Keviczky, T., and de Schutter, B. (2009). Distributed model predictive control of irrigation canals. *Networks and Heterogeneous Media*, 4(2):359–380.

Schuurmans, J., Bosgra, O., and Brouwer, R. (1995). Open-channel flow model approximation for controller design. *Applied Mathematical Modelling*.

Schuurmans, J., Clemmens, J., S.Dijkstra, Hof, A., and Brouwer, R. (1999a). Modeling of irrigation and drainage canals for controller design. *Journal of Irrigation and Drainage Engineering*, 125(6):338–344.

Schuurmans, J., Hof, A., S.Dijkstra, Bosgra, O., and Brouwer, R. (1999b). Simple water level controller for irrigation and drainage canals. *Journal of Irrigation and Drainage Engineering*, 125(4):189–195.

Silva, P., Botto, M. A., and ao Figueiredo, J. (2007). Model predictive control of an experimental canal. In *European Control Conference*, pages 2977–2984, Kos, Greece.

Szymkiewicz, R. (2010). *Numerical Modeling in Open Channel*. Springer-Verlag.

van Overloop, P. (2006). *Model Predictive Control on Open Water Systems*. IOS Press.